scientific reports

Check for updates

OPEN

Multi response optimization in MQL milling of GTD450 stainless steel using an integrated Taguchi grey relational analysis

Masoud Saberi[1], Seyed Ali Niknam[1]✉, Ali Hajaliakbari[2], Behnam Davoodi[1] & Ramin Hashemi[1]

The GTD450 stainless steel is highly valued in aerospace and turbine applications for its exceptional mechanical and thermal properties; however, its low machinability and the scarcity of data on optimal cutting and lubrication conditions present a significant industrial challenge. While the environmentally friendly Minimum Quantity Lubrication (MQL) method is a promising candidate for machining this alloy, a comprehensive study on the application and optimization of its key parameters—specifically oil concentration and spray pressure, in conjunction with standard cutting variables—was absent. To address this research gap, this study employed a Taguchi L25 orthogonal array to experimentally investigate the simultaneous effects of these parameters. The results demonstrated that fluid concentration improved surface roughness by up to 12%, while MQL pressure reduced tool wear by up to 37.5%. Furthermore, multi-objective optimization using the Grey Relational Grade (GRG) method yielded a 38.8% improvement in the overall performance index, identifying the optimal parameter set as follows: 15% concentration, 900 mm/min feed rate, 180 m/min cutting speed, 1.5 mm depth of cut, and 10 bar pressure. These significant findings are now being successfully implemented in relevant manufacturing sectors.

Keywords GTD450, Minimum quantity lubrication (MQL), Surface roughness, Flank wear, Grey relational analysis, Grey relational degree

Abbreviations

MQL	Minimum quantity lubrication
MRR	Material removal rate
GRA	Gray relational analysis
GRG	Gray relational grade
VB	Flank wear
C	Oil concentration
Vc	Cutting speed
Fm	Feed rate
Ap	Depth of cut
P	Pressure
Ae	Width of cut
Ra	Average surface roughness

GTD450 is a martensitic precipitation-hardening stainless steel[1] with exceptional characteristics, including good corrosion resistance, high strength at temperatures below 500 °C, and high toughness[2]. It is widely used in various industries due to its excellent mechanical and thermal properties, particularly in the production of jet engines and gas turbine parts[3]. This alloy is suitable for harsh conditions due to its high temperature and corrosion resistance. The unique characteristics of this material include high heat resistance, corrosion resistance, and excellent mechanical properties[4,5]. Despite the mechanical and thermal properties of this superalloy, machining this material presents challenges. Despite recorded works on the machining of superalloys[6–8], limited studies

[1]School of Mechanical Engineering, Iran University of Science and Technology (IUST), Tehran, Iran. [2]MAPNA Group, TUGA, Tehran, Iran. ✉email: saniknam@iust.ac.ir

have been reported on the machining of GTD450 stainless steel. This indicates the importance of research in GTD450 machining.

In the current era, when environmental issues are of critical importance, process optimization in industry is particularly significant. New methods have been increasingly considered to reduce resource consumption, improve operator health, and protect the environment. One of these methods is the MQL method, which is primarily used in machining. In the MQL machining, tiny amounts of lubricants are used during the machining process, and it is injected into the cutting area at very low pressure, which helps reduce the temperature in the cutting area and provides lubrication properties[9,10]. This technique has been specifically developed to minimize industrial oil consumption and improve machining efficiency[11,12]. Given that a large volume of cutting oils is wasted in machining processes, leading to environmental pollution, using optimized methods such as MQL is considered a sustainable and practical solution[13–15]. Since high friction in the cutting zone generates a significant amount of heat, it accelerates the wear rate, reduces tool life, limits cutting conditions, and necessitates the use of high-quality cutting inserts[16]. MQL can reduce or even eliminate heat and temperature in the cutting zone[17]. Research studies have shown that this method can increase tool life, reduce wear, and improve the surface quality of parts. Reported studies indicate that combining vegetable oils with the MQL technique optimizes machining performance, ultimately reducing negative environmental impacts[18,19]. Ongoing research works in MQL areas are presented in Fig. 1.

Many types of cutting fluids, such as distilled water, oil-in-water emulsion, vegetable oil, etc., have been studied and used, among which vegetable oils are the most promising alternative solution for the MQL method because they have many advantages, such as high viscosity, biodegradability, non-toxicity, and environmentally friendly properties[20,21]. The following passages present the main types of lubricants used in machining operations.

Vegetable oil-based

Vegetable oil-based machining fluids have been used to study the performance of cutting force, workpiece surface finish, tool wear, and cutting zone temperature in machining various materials[22]. Saravanan et al. utilized non-edible vegetable oil cooling in ANSI 1050 drilling and examined its stability and impact on tool wear, surface roughness, and cutting force[23]. Compared to dry cutting, the combination of castor oil and MQL increased the life of carbide-coated tools[24]. Peanut oil reduced the cutting force by approximately 51% and decreased tool vibration during aluminum machining[25]. Rice bran oil reduced tool tip temperature, surface roughness, and cutting forces with minimal lubrication during the machining of AISI 304 stainless steel[26]. Figure 2 presents the types of vegetable oils used in machining.

Oil mist

It refers to a machining process that uses a minimum amount of cutting fluid or coolant. In near-dry machining, a small amount of coolant is applied to the cutting zone, usually as a mist or vapor, to provide lubrication and cooling. However, the amount of coolant used is much lower than that of traditional flood cooling methods. Near-dry machining aims to strike a balance between the advantages of cutting fluids for lubrication and cooling, and the disadvantages associated with excessive fluid use, including environmental concerns, cleanup, and increased costs[27]. Obikawa et al. investigated the performance of oil mist sprays in the machining of Inconel 718. The results exhibited that reducing the distance from the outlet of a nozzle to the tool tip increased the pressure and velocity of the compressed air, thereby increasing the flow rate of the compressed air[28].

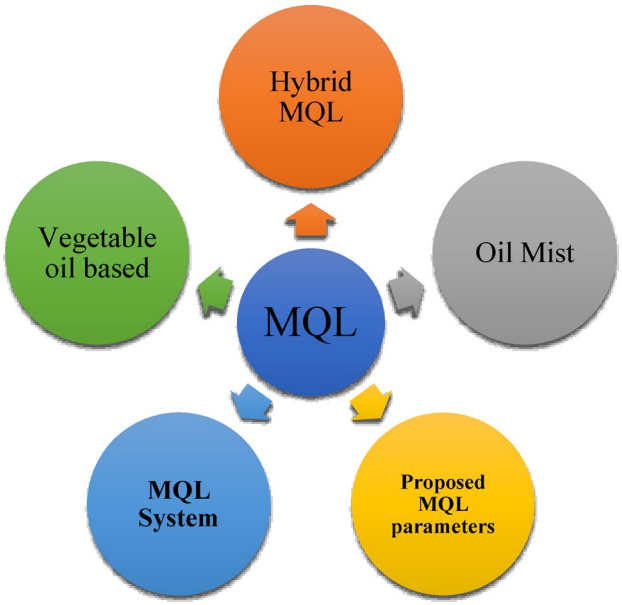

Fig. 1. MQL and various research areas in this field.

Fig. 2. Vegetable oils that have been studied in research[27].

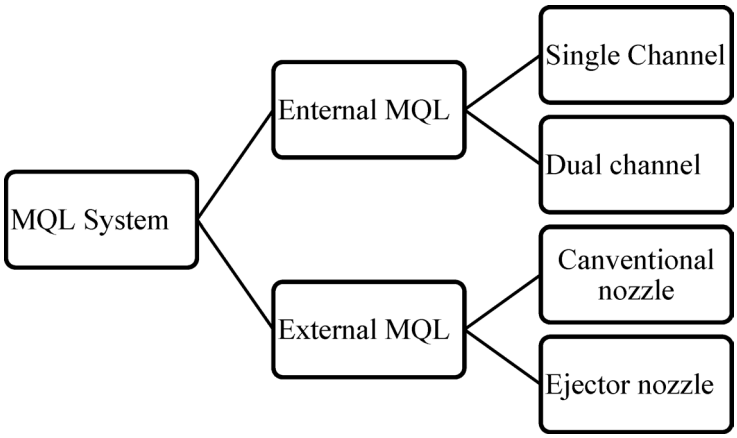

Fig. 3. Classification of MQL system types.

MQL hybrid

This method combines the MQL strategy with or alongside another cooling method. These studies include cryogenic MQL, nanofluid MQL, hybrid nanofluid MQL, and ultrasonic vibration-assisted MQL[29]. Many studies have acknowledged the positive effect of the hybrid method on surface integrity tool life[12,30]. Attempts have been made to combine two or three coolant solutions to enhance the effects of cooling and lubrication methods in machining operations. In the machining of Inconel alloy, the combination of cryogenic and MQL techniques increased surface roughness by 18% and nearly doubled tool life[31]. Unlike other lubricants, hybrid coolants offer promising results in machining efficiency. In the case of other cutting fluids, hybrid nano-green fluids at a concentration of 0.3% improved cutting power, feed force, friction coefficient (at the interface between the tool and workpiece), and surface roughness[32]. Pereira et al.[33] Their research showed that using the Cryo-MQL method to drill holes by helical milling in Inconel 718 increased the life of the cutting tool. In summary, compared to dry machining, it significantly reduced cutting forces by 33%, improved Ra by 46%, and reduced material adhesion to the tool, with 31% of material adhesion in Cryo-MQL compared to 87% in dry machining[34].

MQL supply systems

A commercial MQL system typically consists of five main components: an air compressor, a cutting fluid reservoir, pipes, a flow control system, and a spray nozzle[35]. The types and classification of MQL systems are shown in Fig. 3. Zeilmann and Weingaertner[36] investigated the machining performance of external and internal MQL drilling on Ti-6Al-4 V titanium alloy by measuring the drilling temperature. They reported that internal MQL drilling resulted in a 50% lower maximum temperature rise compared to external MQL. This is due to the lack of aerosol penetration into the hole during the machining process. On the other hand, the short aerosol travel distance of a dual-channel internal MQL gives it an advantage because the oil and pressurized air are mixed close to the cutting tool, causing the mixture to be affected by the spindle rotation for only a short time. As

a result, this reduces the dispersion and fallout of the discharged aerosol, and the mist produced contains larger droplets than droplets from external MQL[37]. The researchers concluded that the dual-channel internal MQL system is the most effective method among the methods mentioned earlier[38].

Proposed MQL parameters

Sarma et al.[39] optimized the machining of Ti6Al4V using MQL. Parametric analysis showed that feed has the most significant effect on Ra, followed by cutting speed and depth of cut. Jouini[14] optimized the machining of turning using MQL. Multi-objective optimization using gray relational analysis (GRA) identified the optimal machining parameters for AISI 4340 alloy. Subsequently, the Cryogenic + MQL technique was applied to these parameters. It yielded significant improvements, with a 48% reduction in surface roughness and a 184.5% increase in tool life, which was attributed to improved lubrication and cooling efficiency. However, a slight increase of 4.6% in cutting force was observed, probably due to the surface hardening caused by the low-temperature LN2 cooling. Furthermore, reducing tool sticking and breakage at the leading cutting edge under Cryogenic + MQL conditions justifies the superior surface quality and increased tool life. This research highlights the industrial importance of hybrid lubrication in addressing the challenges associated with hard-turning processes. Liu et al.[40]. The results suggest that, using MQL, the contributions of cutting speed and air pressure to the dust particle diameter were 54.62% and 25.34%, respectively. Increasing air pressure increased the overall proportion of dust particles with diameters in the 2.5–10 μm range, from 88 to 96%.

Modern technological advances have led to innovations in incorporating nanoparticles into base fluids, enhancing the properties and performance of cutting fluids. This technology is called nanofluids. Nanoparticle-based fluids are defined as new fluids resulting from the dispersion of nanoparticles with a size of less than 100 nm in the base fluid of the cutting fluid. The nanoparticles used typically vary depending on the application requirements and exhibit good stability, as well as high thermal conductivity. In the scientific community, nanofluids are recognized for improving cutting efficiency when they serve as the lubricant, unlike other lubrication techniques. These nanoparticles include metal oxides (Al_2O_3, TiO_2, CuO, SiO, Fe_2O_3, ZnO), various metal nitrides (SiN, AlN, hBN), various metal carbides (SiC), carbon (graphite, CNT, MWCNT)[41]. Gajrani et al.[42] used calcium disulfide and molybdenum disulfide for machining hardened steel with tungsten tools. The result showed an 11.01% reduction in friction between the workpiece and the tool. Zaman et al.[43] optimized the parameters in machining Ti-6Al-4 V using Al_2O_3-MWCNT nanoparticles. Kumar et al.[44]. Found that using MQL can be a suitable alternative to flood lubrication, facilitating environmentally friendly machining. To achieve better results, optimization of MQL parameters is needed in future research. MQL requires further optimization to create ideal conditions, such as the nozzle location in relation to the cutting tool, the coolant flow rate, the nozzle distance from the tool, and the pressure range[21]. Non-toxic and environmentally friendly cutting fluids, MQL-assisted machining methods, and other sustainable machining methods will be the options for future machining technology.

There are still many gaps in our understanding of many aspects of MQL machining that require further study[27]. A review of the research conducted, as mentioned, highlights the importance of the MQL method, which warrants further investigation and the overcoming of existing challenges. One of the challenges is selecting the optimal parameters. Most of the research has focused on the three parameters of cutting speed, feed, and depth of cut, as well as the effects of oil and nanoparticles. In contrast, the study and investigation of MQL parameters have been relatively limited. Hence, this research simultaneously investigates both the cutting parameters and the concentration and pressure parameters of the MQL nozzle. In addition to the reasons mentioned, there is very little literature on GTD450 machining, and, given its numerous and specialized applications, further research is warranted.

Two primary objectives drive this study. First, it aims to address the significant research gap regarding the machinability of GTD450 stainless steel, a material critical to high-performance industries that has been scarcely studied from a manufacturing standpoint. Second, it aims to investigate under-examined Minimum Quantity Lubrication (MQL) parameters—specifically, oil pressure and concentration—moving beyond the well-documented nozzle configuration parameters (e.g., angle and spacing). The ultimate goal is to develop an optimized and sustainable machining strategy for this challenging material using MQL.

Experimental design

The workpiece was a nickel-based superalloy, GTD-450, with dimensions of 65 × 85 × 320 mm. Additional information about the material and its constituent elements in GTD 450 is presented in Tables 1 and 2. The cutting speed, feed, depth of cut, lubricant concentration, pressure, and MQL spray flow rate were evaluated at five levels (Table 3). The Taguchi L25 method was used in the experimental design (Table 4).

Experimental tools/apparatus

The milling experiment was performed on a 5-axis CNC machine. The tool used is a 63 mm diameter insert tool with a coated insert, featuring a rake angle of 16° and a clearance angle of 11°. The setup used is illustrated in Fig. 4. This current study thoroughly analyzed surface roughness, a crucial parameter in evaluating surface quality. After conducting each test, we measured the average surface roughness (Ra) values.

Tensile strength	Yield strength	Hardness	Elongation	Density	Melting temperature
1010–1250 Mpa	910 Mpa	302-363BHN	16%	7.78 g/cm^3	1400–1450 °C

Table 1. Mechanical properties of GTD450.

Weight%																
C	Mg	Ni	Cr	Mo	P	S	S	Cu	Nb	V	Sn	Al	Pb	Ag	N	Fe
0.035	1	6.5	15	0.75	0.025	0.005	1	1.5	0.55	0.1	0.005	0.05	0.1	0.005	0.03	Balance

Table 2. Chemical composition of GTD450.

Run order	C(%)	Vc (m/s)	Fm (mm/min)	Ap (mm)	P (bar)
1	5	180	900	0.5	6
2	5	190	950	0.75	7
3	5	200	1000	1	8
4	5	210	1050	1.25	9
5	5	220	1100	1.5	10
6	10	180	950	1	9
7	10	190	1000	1.25	10
8	10	200	1050	1.5	6
9	10	210	1100	0.5	7
10	10	220	900	0.75	8
11	15	180	1000	1.5	7
12	15	190	1050	0.5	8
13	15	200	1100	0.75	9
14	15	210	900	1	10
15	15	220	950	1.25	6
16	20	180	1050	0.75	10
17	20	190	1100	1	6
18	20	200	900	1.25	7
19	20	210	950	1.5	8
20	20	220	1000	0.5	9
21	25	180	1100	1.25	8
22	25	190	900	1.5	9
23	25	200	950	0.5	10
24	25	210	1000	0.75	6
25	25	220	1050	1	7

Table 3. The experimental milling conditions.

Item	
Cutting insert	Coated carbide, RPHT1204M0T-6-M08-MS2500 ($TiCN + Al_2O_3$)
Tool holder working tool geometry	HSK, R220.29I-0063–06.6A
Working tool geometry	Clearance angle: 11°
	Rake angle: 16°
Process parameters	
Cutting speed (Vc)	180, 190, 200, 210, 220 m/s
Feed rate (Fm)	900, 950, 1000, 1050, 1100 mm/min
Depth of cut (Ap)	0.5, 0.75, 1, 1.25, 1.5 mm
Concentration	5, 10, 15, 20, 25%
Pressure	6, 7, 8, 9, 10 bar
Nozzle angle	30°
Nozzle distance	20 mm

Table 4. Milling machine parameter.

To evaluate machining performance, surface roughness was measured immediately after each test using a MarSurf PS 10 profilometer. Multiple measurements were taken across the workpiece to ensure reliability, with the results averaged for consistency. A key challenge observed was rapid tool wear, particularly with difficult-to-machine materials, which detrimentally affects both machining efficiency and workpiece surface quality. To quantify this, tool wear was documented according to the conditions in Table 4, using the average flank wear width (VBavg) as the primary metric for tool longevity and wear rate analysis. This involved removing the inserts after each operation, imaging them with an SEM microscope, and calculating the average wear. Furthermore, the metal removal rate was identified as a critical parameter for productivity, defined as the volume of material removed per unit time and calculated using the standard milling formula provided in Eq. 1.

$$\mathrm{MRR} = \frac{(\mathrm{Fm} \times \mathrm{Ap} \times \mathrm{Ae})}{1000} \tag{1}$$

Fm = Feed rate (mm/min); Ap = depth of cut (mm); Ae = width of cut (mm).

Results and discussion

This section analyzes the results of machining tests performed under different lubrication conditions and presents the statistical analysis for each experimental model. A multivariate regression model, which perfectly fit the data, was used to evaluate the effects of key parameters, their squared terms, and their two-way interactions. The study employed a 95% confidence level for all experimental design analyses.

Statistical analysis of flank wear

Tool wear is a vital machinability indicator, especially for challenging materials like GTD450, as it directly impacts surface quality, cutting forces, and tool longevity. This study considered both MQL parameters (concentration and pressure) and standard cutting parameters (speed, feed rate, depth of cut) as inputs. After machining, the GTD450 inserts were examined using electron microscopy to analyze the wear mechanisms. A

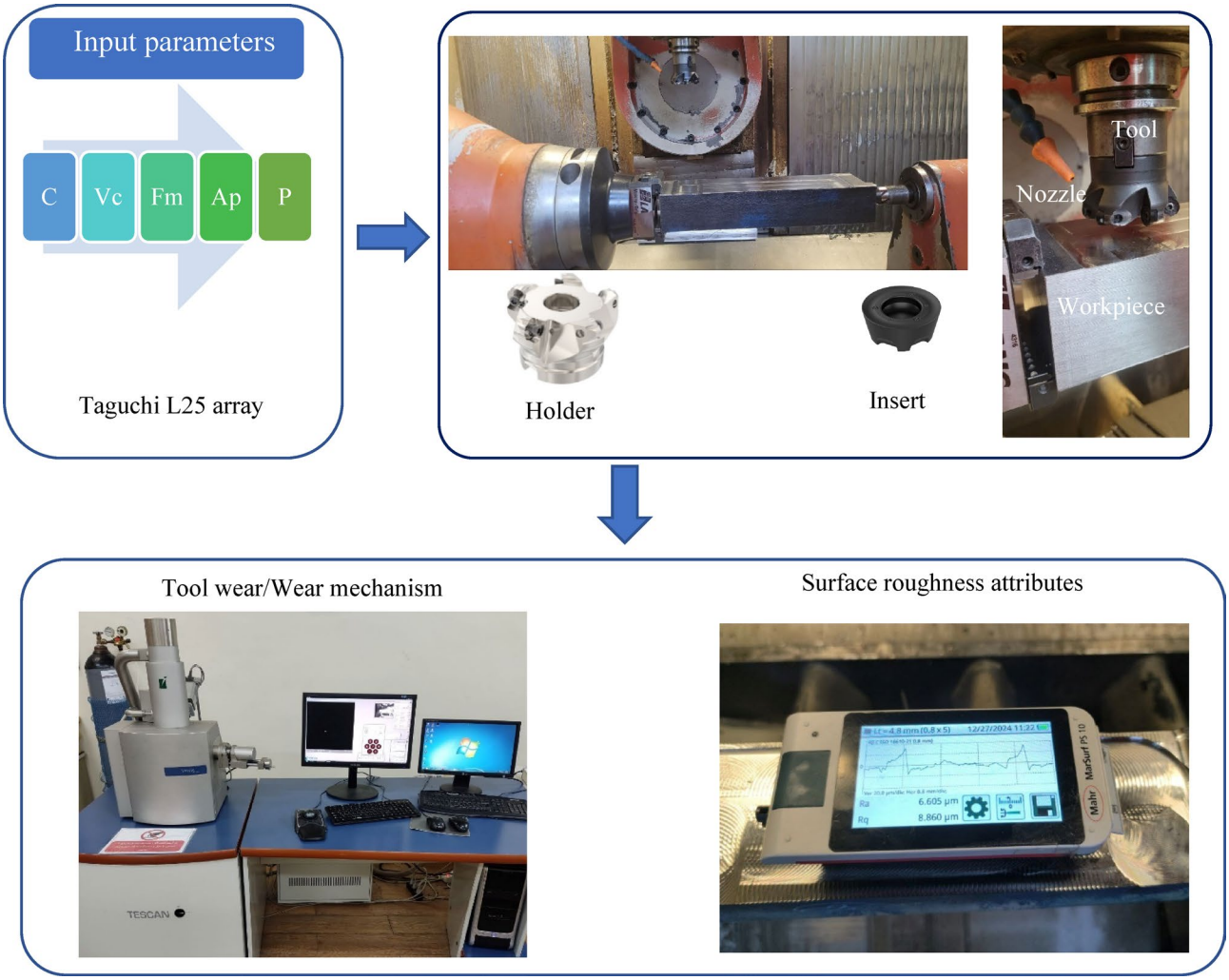

Fig. 4. Experimental setup, input variables, and output machinability parameters.

primary challenge is the high temperatures generated, which hinder heat dissipation, increase friction, and lead to material adhesion, forming a built-up edge. Furthermore, the hard alloying elements, such as chromium, nickel, and vanadium, in GTD450 cause significant abrasive wear on the tool. Consequently, effective heat control is crucial. The analysis revealed flank and rake wear, with mechanisms dominated by abrasion and built-up edge formation. The average flank wear (VBavg) was measured to quantify the total wear (Fig. 5).

Figure 6 displays a 3D surface chart illustrating the effects of various parameters on tool life. Cutting speed has a direct relationship with tool wear: as cutting speed increases, wear also increases, leading to a reduction in tool life. According to research and studies, cutting speed has the most significant impact on wear and tool lifespan[45,46]. Increasing the cutting speed raises the temperature in the cutting zone, which reduces the shear edge strength and accelerates tool wear. Tool wear in machining processes is unavoidable; however, by adjusting input parameters appropriately and utilizing effective cooling and lubrication methods, its progression can be slowed down. Increasing the concentration at a fixed cutting speed decreases wear (up to 20%), but at 25%, wear increases again (Fig. 6a). Since the oil and water mixture serves as a lubricant and a coolant, increasing the oil concentration initially improves lubrication and reduces friction. However, the water content decreases beyond a specific concentration (15%), reducing the cooling effectiveness, which in turn increases wear. Figure 6b shows that increasing concentration reduces tool wear at lower feed rates; however, it causes surface roughness to increase at higher feed rates. This is because the fluid spray has less of an opportunity to penetrate the cutting zone at higher feed rates. According to Fig. 6c at shallow depths of cut, increasing concentration reduces wear. However, at greater depths of cut, since the engagement between the tool edge and the workpiece is higher, increased concentration leads to higher viscosity, which reduces the chances of fluid penetration and, consequently, wear increases. The chart in Fig. 6d shows that increasing pressure (with the flow rate remaining stable) causes flank wear to increase at a constant concentration. However, at a fixed pressure, increasing concentration initially leads to a slight improvement in wear, but then wear increases again. In Fig. 6e, f, h, the data demonstrate that, overall, cutting speed, feed rate, and depth of cut have a direct relationship with tool wear. Keeping each parameter constant while increasing the others results in increased wear, precisely consistent with Taylor's relation and its extended form. In Fig. 6g, at a constant cutting speed, increasing pressure results in greater tool wear. This can be explained by the fact that, with increasing pressure (and a constant fluid flow rate), higher pressure results in less lubricant reaching the cutting zone at any given moment, thereby increasing wear. The same reasoning applies to Fig. 6i, j, where the depth of cut and feed rate are held constant.

Statistical analysis of average surface roughness (Ra)

Surface roughness is another vital machinability attribute that significantly impacts the performance of the manufactured part. It is one of the essential requirements for partial production. Therefore, by understanding the factors affecting this output, we can help reduce manufacturing costs and improve the quality of the parts. Since machining parameters influence surface roughness, this study focuses on investigating and analyzing the effects of these parameters on the finished surface roughness. Figure 7a shows that increasing the concentration reduces surface roughness at low cutting speeds because lubrication is more effective. However, due to increased temperature in the cutting zone, the effect of concentration on roughness becomes less significant at higher cutting speeds. Figure 7b indicates that feed rate and surface roughness have a direct relationship. Increasing concentration at all feed rates results in higher surface roughness because the tool covers a greater distance per

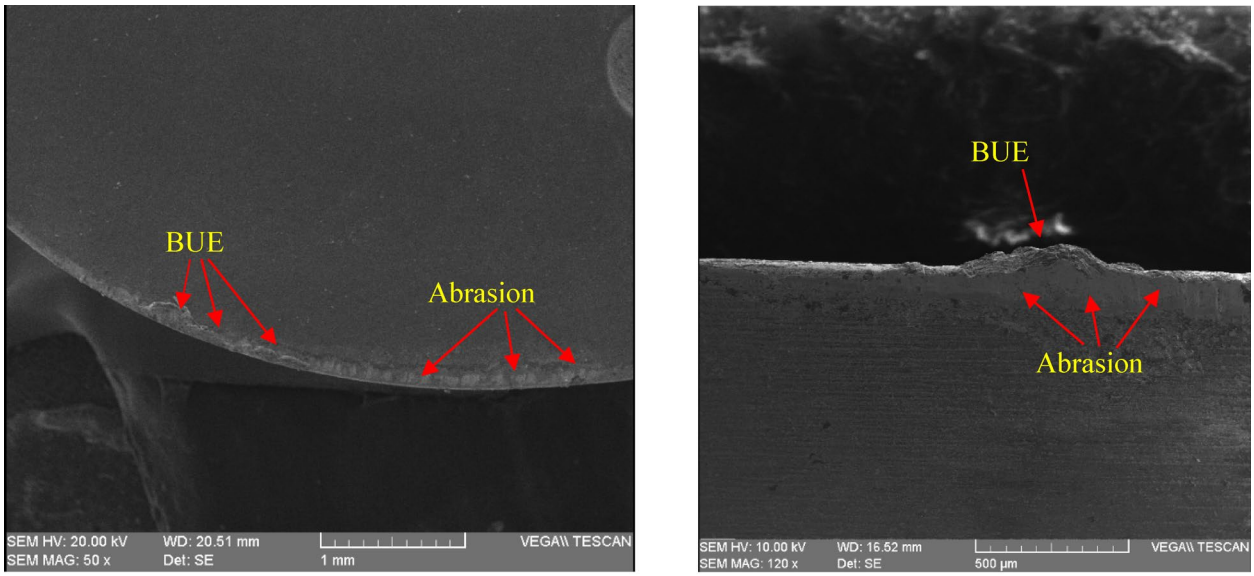

(a) Rake face (b) Flank face

Fig. 5. SEM image of tool wear in test 1.

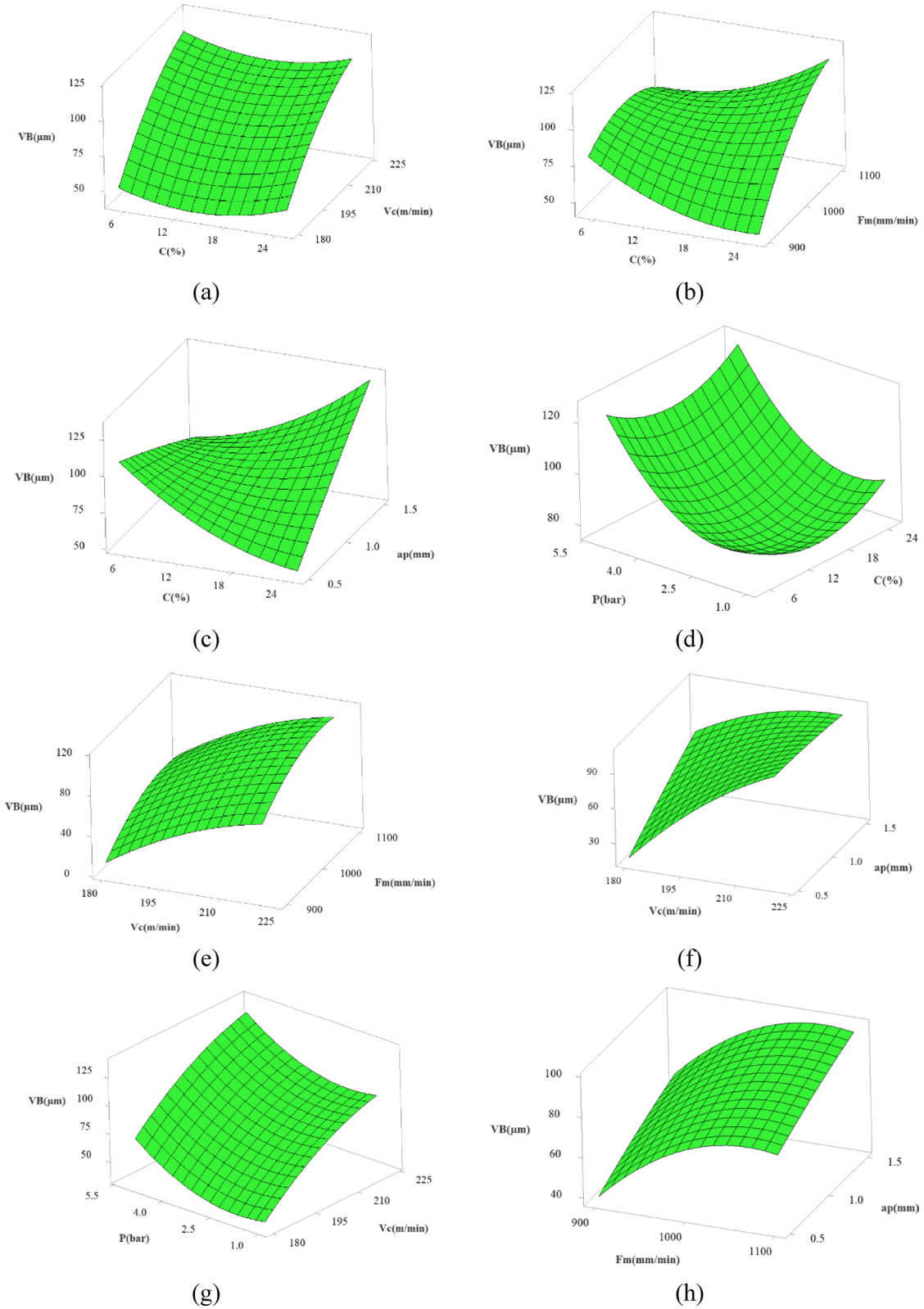

Fig. 6. 3D diagram of input parameters and flank wear.

revolution. Figure 7c shows the interaction effect of concentration and depth of cut on surface roughness. In this chart, increasing the depth of cut at lower concentrations leads to higher roughness. This is because the longer contact length of the tool edge with the workpiece, combined with lower concentration, results in less effective lubrication. Conversely, at higher depths of cut and higher concentrations, the surface roughness is

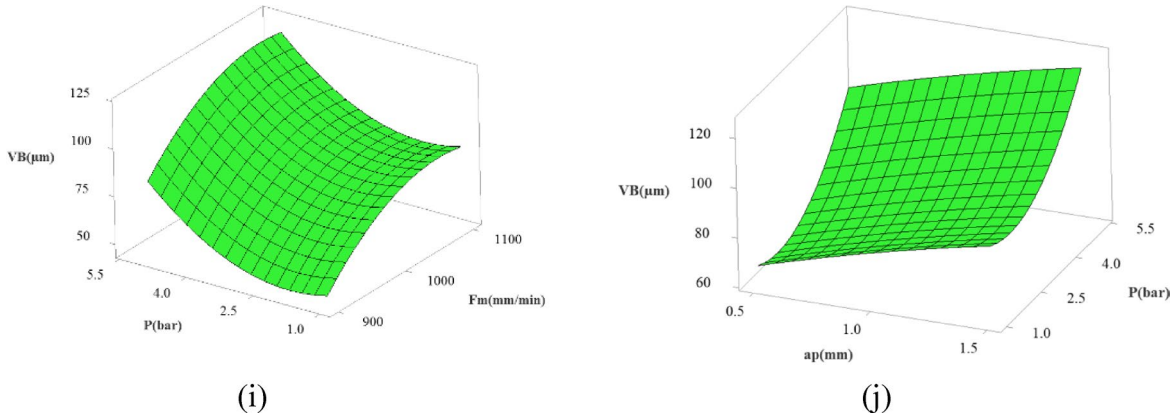

Fig. 6. (continued)

lower. Figure 7d shows that increasing pressure improves surface roughness, as better lubricant penetration in the cutting zone reduces roughness.

Surface roughness has a direct relationship with feed rate and an inverse relationship with cutting speed, with the key difference that feed rate has a greater influence on roughness (Fig. 7e). At a constant cutting speed, increasing the depth of the cut has little to no significant effect on surface roughness. This point is evident in Fig. 7f. In Fig. 7g, increasing the cutting speed at a fixed pressure results in a decrease in surface roughness. Furthermore, at higher cutting speeds, increasing pressure results in reduced roughness because, with a constant flow rate, less lubricant is injected into the cutting zone per unit time. According to (Fig. 7h), at a constant depth of cut, increasing feed rate causes higher roughness due to the tool covering a longer distance per revolution, creating taller peaks that increase the roughness number. Conversely, changing the depth of cut at a constant feed rate does not significantly affect these peaks; hence, it has no impact on roughness. Figure 7i illustrates that surface roughness is directly related to the feed rate at a constant pressure.

In contrast, in a fixed feed rate scenario, changes in pressure have a negligible effect on roughness. Finally, the chart in Fig. 7j shows that each depth of cut has an optimal pressure at which the roughness index is maximized. Initially, increasing pressure increases roughness, but it decreases again after reaching its maximum point. This pattern holds across different fixed depths of cut.

Response surface regression-based modeling

Response surface methodology is a set of mathematical and statistical techniques for modeling and analyzing problems based on the statistical design of experiments and least squares fitting. Several input variables influence the response, and the goal is to identify a correlation between the response and the variables under study[47]. A regression is performed on the collected data in which the observed variable is approximated based on a functional relationship between the estimated variable and one or more input variables. The second-order response surface, which represents the output (Y), can be expressed as a function of cutting parameters, including C, Vc, Fm, Ap, and P. The relationship between the output and machining parameters is described as follows:

$$\begin{aligned} Y = {} & \beta_0 + \beta_1 (C) + \beta_2 (Vc) + \beta_3 (Fm) + \beta_4 (Ap) + \beta_5 (P) + \beta_6 \left(C^2\right) \\ & + \beta_7 \left(Vc^2\right) + \beta_8 \left(Fm^2\right) + \beta_9 \left(Ap^2\right) + \beta_{10} \left(P^2\right) + \beta_{11} (C \times Vc) \\ & + \beta_{12} (C \times Fm) + \beta_{13} (C \times Ap) + \beta_{14} (C \times P) + \beta_{15} (Vc \times Fm) + \beta_{16} (Vc \times Ap) \\ & + \beta_{17} (Vc \times P) + \beta_{18} (Fm \times Ap) + \beta_{19} (Fm \times P) + \beta_{20} (Ap \times P) \end{aligned}$$

where Y is the corresponding response, β0 is a constant called the width from the origin of the plate, and β1, β2,…, β20 are regression coefficients that depend on the main effects. The β coefficients in Eq. (1) can be calculated using least squares techniques. The terms C, Vc, Fm, Ap, and P are the input variables, C2, Vc^2, Fm^2, Ap^2, and P2 are the quadratic terms, and C × Vc, C × Fm, C × Ap, C × P, and… to Ap × P are the interaction terms for the input variables, respectively. The second-order model is usually used when the response function is unknown or nonlinear. The regression equation and the coefficient of determination (R^2) were calculated to test the model's fit, and acceptance was based on the high correlation coefficient (R^2). It also indicates the extent to which the model explains the variation in the response. The relationship between the parameters affecting surface roughness (R2 = 96.59%) is shown in the following equation:

$$\begin{aligned} Ra = {} & 7.39 - 0.1301\ C - 0.0975\ Vc + 0.00914\ Fm - 0.0151\ Ap - 0.0081\ P \\ & + 0.000203\ Vc^2 - 0.000003\ Fm^2 + 0.000610\ C \times Vc. \end{aligned}$$

The relationship between the parameters affecting sidewall wear (R2 = 97.6%) is shown in the equation below:

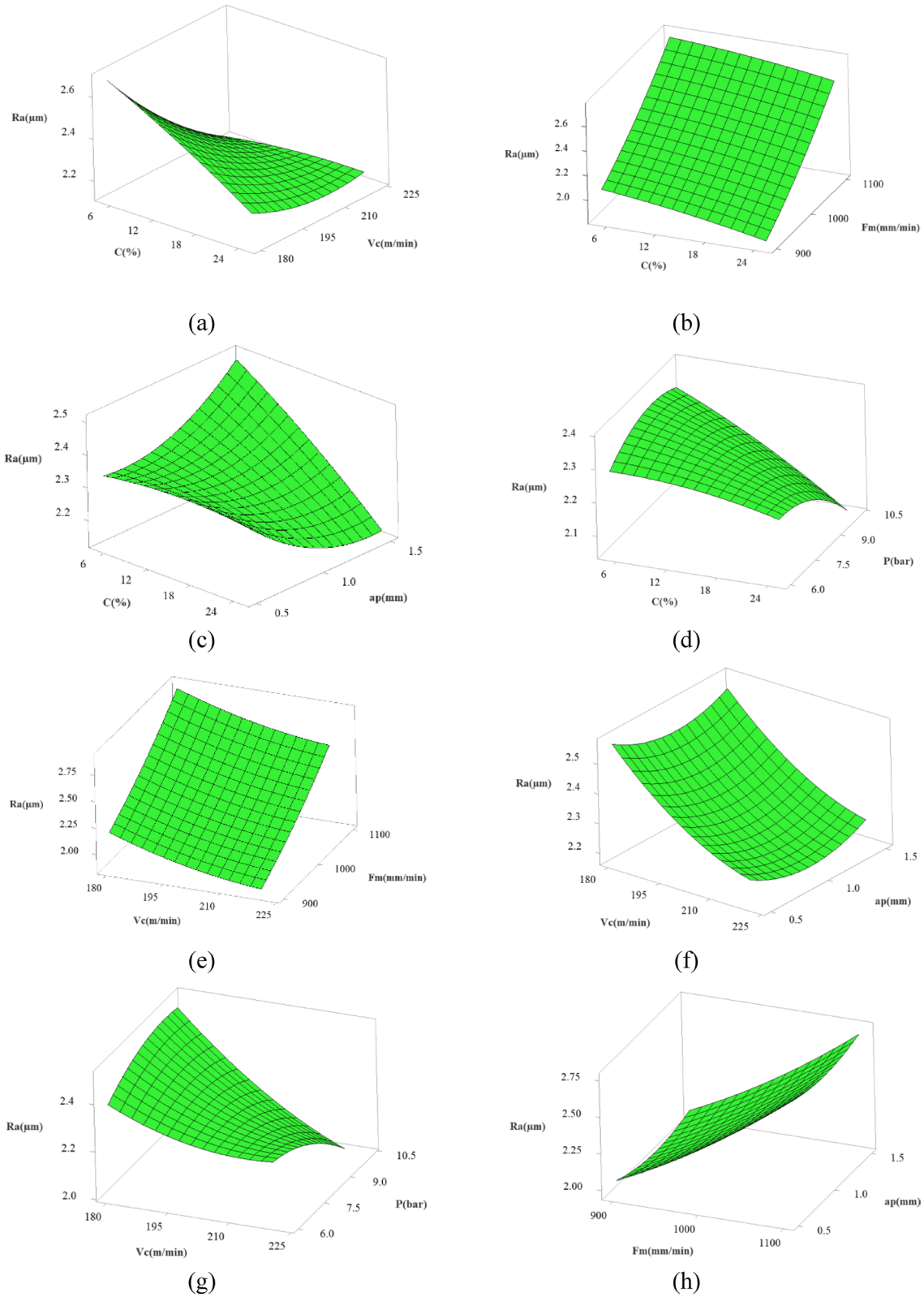

Fig. 7. 3D diagram of input parameters and surface roughness (Ra).

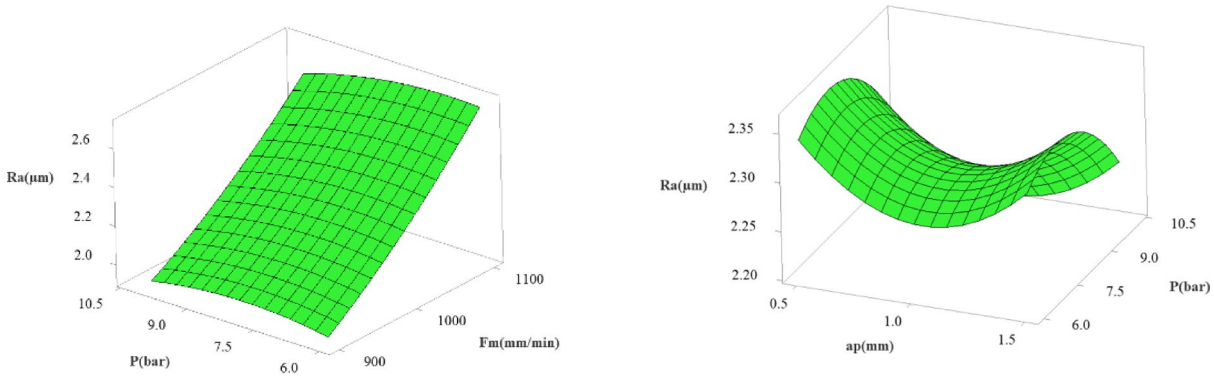

Fig. 7. (continued)

$$\mathrm{VB} = -340.5 + 2.12\ \mathrm{C} + 0.965\ \mathrm{Vc} + 0.2177\ \mathrm{Fm} - 32.3\ \mathrm{Ap} + 35.3\ \mathrm{P} + 0.0814\ \mathrm{C} \times \mathrm{C} + 15.47\ \mathrm{Ap}^2 - 0.763\ \mathrm{P} \times \mathrm{P} - 0.02152\ \mathrm{C} \times \mathrm{Vc} - 0.02298\ \mathrm{Fm} \times \mathrm{P}.$$

The Pareto diagram shows the effect of each parameter on the output. In other words, the parameters can be examined in order of importance, allowing for a comparison of the effect of each parameter. Figure 8a shows the beam diagram related to surface roughness. According to this diagram, the feed has the most significant effect on surface roughness, followed by cutting speed and concentration in that order. The cutting speed has shown the most impact on the life of the cutting tool (Fig. 8b).

Multi-response optimization using grey relational analysis (GRA)

Various methods are used to optimize several output parameters. One of these methods is the gray relational analysis method, which is based on the Taguchi method. Gray relational analysis was introduced by Deng in 1982. The effectiveness of this method in dealing with uncertainty and insufficient information has been proven. Gray relational analysis has also been used to solve various multi-attribute decision-making problems in many specialized and general management fields. One of the advantages of gray relational analysis compared to other multi-attribute decision-making methods is that it has no restriction on the sample size or normality of the data distribution. Additionally, its computational method is straightforward to use. It is a measurement method for determining the degree of approximation between sequences using the gray relational degree (GRG). The steps of gray relational analysis are shown in Fig. 9.

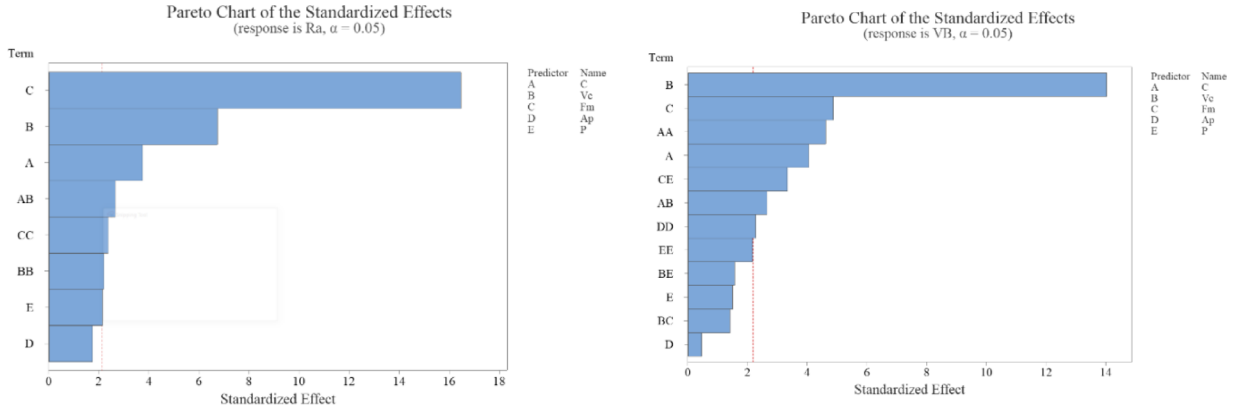

Fig. 8. Tool wear and surface roughness pareto diagram after removing ineffective parameters.

This paper used GRG to determine the optimal combination of milling parameters that simultaneously minimizes two responses, VBavg and Ra. After normalizing the experimental results, GRG was determined to evaluate multiple responses to achieve this goal. In GRA, the first step is to normalize the experimental data to create a range in 0–1. This step is referred to as the generation of the gray relation. Considering the importance of qualitative features, it can be divided into three criteria for optimization in GRA, namely "bigger-better" , "smaller-better" and "nominal-best"[48]. If the expectation is bigger-better, the normalized value of the gray relation can be described by Eq. 2:

$$x_i(k) = \frac{x_i^o(k) - \min\left(x_i^0(k)\right)}{\max(x_i^0(k) - \min(x_i^0(k))}. \tag{2}$$

If the objective is nominal-better, the normalized value of the gray relation can be obtained in the Eq. 3:

$$x_i(k) = 1 - \frac{\left|x_i^0(k) - OA\right|}{\max\left[\max\left((x_i^0(k)) - OA, OA - \min(x_i^0(k))\right)\right]} \tag{3}$$

here OA is the target value.

In this paper, the smaller the value of tool wear patterns and the lower the surface roughness, the more desirable. Therefore, the "smaller is better" calculation method was used because it is considered to minimize VBavg and Ra. Therefore, smaller-is-better should be explained in the Eq. 4:

$$x_i(k) = \frac{max\left(x_i^0(k)\right) - x_i^0(k)}{\max(x_i^0(k) - \min(x_i^0(k))} \tag{4}$$

where $x_i(k)$ is the value after generating the gray relation. And $\max(x_i(k))$ and $\min(x_i(k))$ are the maximum and minimum values of $x_i(k)$ respectively. In this report, the number of tests ranges from 0 to 25. All the

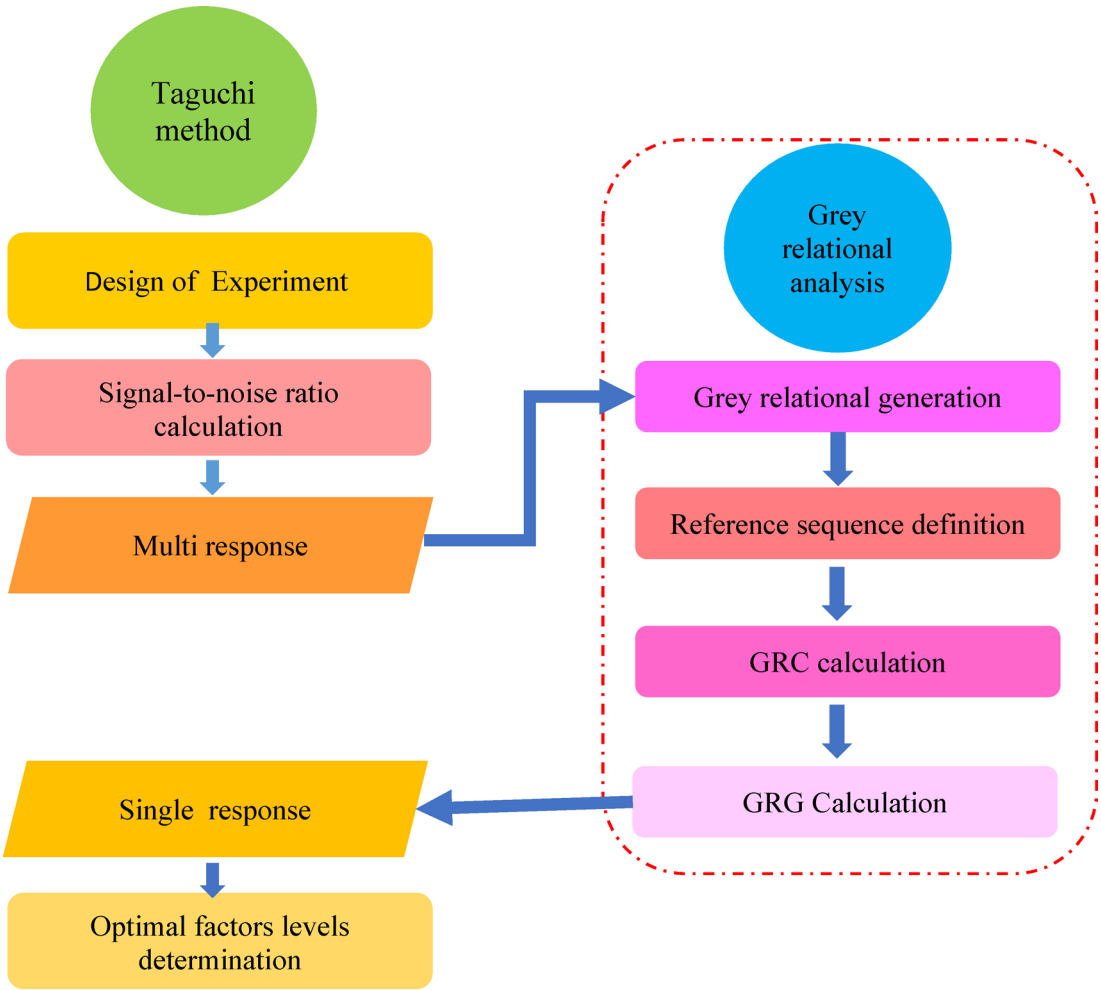

Fig. 9. Flowchart of optimization steps.

sequences after applying the data preprocessing through Eq. (3) are shown in Table 6. In fact, larger normalized results are expected to yield better performance. The best-normalized result should be equal to one. In addition, the gray relation coefficient (xi (k)) is assigned to explain the relationship between the desired and actual experimental normalized data. The gray relation coefficient is defined as follows:

$$\xi_i(k) = \frac{\Delta_{min} + \lambda\Delta_{max}}{\Delta_{oi}(k) + \lambda\Delta_{max}} \tag{5}$$

where = $\Delta_{0i}(k) = x_0^*(k) - x_i^*(k)$ is the absolute difference between × 0(k) and xi(k), Δ_{min} and Δ_{max} are the minimum and maximum absolute difference values of all the comparing sequences, respectively. ζ is the discrimination or identification coefficient, and its value is between 0 and 1 ($0 \le \lambda < 1$), which aims to weaken the influence of Δ_{max} When it becomes too large, the significance of the difference in the correlation coefficient increases. Generally, the discrimination coefficient is typically set at 0.5 to meet practical requirements. Therefore, in the present study, λ was taken as 0.5. The Gray correlation coefficients were calculated using Eq. (4), and Table 5 lists these coefficients. Then, the Gray correlation coefficient GRG expresses the correlation level between the reference and the comparable sequence. GRG is the weighted sum of Gray correlation coefficients and is calculated as follows:

$$\gamma_i = \frac{1}{n}\sum_{k=1}^{n}\xi(k) \tag{6}$$

here n represents the number of performance characteristics (in this paper, n = 3). A higher GRG value is considered to have a stronger relationship between the ideal normalized value and the experimental value. Therefore, a higher degree of relationship indicates that combining the relevant process parameters is closer to the optimum. In the last step of GRA, Table 5, calculated using Eq. (5), was identified as the highest GRG in the first order. According to the experimental design, Table 5 and Fig. 10 show that the milling parameter setting 14 (test no. 14) has the highest GRG. Therefore, the fourteenth test offers the best multi-functional characteristics among the other tests for determining the minimum simultaneous tool wear and the minimum surface roughness. Additionally, the average GRG for each level of milling process parameters is summarized in Table 5.

	Normalized values		Grey relational coefficient				GRG, S/N ratio and its orders		
	VB (μm)	Ra (μm)	MRR (mm^3/min)	VB	Ra	MRR	GRG	S/N ratio	Order
1	1	0.4891	0	1	0.4946	0.3334	0.6093	− 4.30	5
2	0.8555	0.4603	0.2188	0.7758	0.4809	0.3902	0.5490	− 5.21	12
3	0.4443	0.3682	0.4583	0.4736	0.4418	0.48	0.4651	− 6.65	19
4	0.268	0.3107	0.7187	0.4058	0.4204	0.64	0.4888	− 6.22	15
5	0.1533	0.1381	1	0.3713	0.3671	1	0.5795	− 4.74	9
6	0.9783	0.2359	0.4167	0.9583	0.3955	0.4615	0.6051	− 4.36	6
7	0.7023	0.2992	0.6667	0.6268	0.4164	0.6	0.5477	− 5.23	13
8	0.367	0.1956	0.9375	0.4413	0.3833	0.8889	0.5712	− 4.86	10
9	0.0995	0.0345	0.0833	0.3570	0.3412	0.3529	0.3504	− 9.11	25
10	0.176	0.9551	0.1875	0.3776	0.9176	0.3809	0.5587	− 5.06	11
11	0.912	0.2186	0.875	0.8503	0.3902	0.8	0.6802	− 3.35	2
12	0.7503	0.1381	0.0625	0.6669	0.3671	0.3478	0.4606	− 6.73	20
13	0.6235	0	0.3125	0.5705	0.3334	0.4211	0.4416	− 7.10	21
14	0.461	0.9551	0.375	0.4812	0.9176	0.4445	0.6144	− 4.23	4
15	0.4158	0.8285	0.6146	0.4611	0.7446	0.5647	0.5902	− 4.58	8
16	0.763	0.1158	0.2813	0.6784	0.3610	0.4103	0.4832	− 6.32	17
17	0.674	0.0806	0.5417	0.6053	0.3523	0.5217	0.4931	− 6.14	14
18	0.686	0.9206	0.5625	0.6143	0.8630	0.5334	0.6702	− 3.48	3
19	0.3723	0.6674	0.8125	0.4434	0.6006	0.7273	0.5904	− 4.58	7
20	0.1123	0.5685	0.0417	0.3603	0.5368	0.3429	0.4133	− 7.67	24
21	0.3213	0.0702	0.7708	0.4242	0.3497	0.6857	0.4865	− 6.26	16
22	0.402	1	0.75	0.4554	1	0.667	0.7073	− 3.01	1
23	0.306	0.7480	0.0208	0.4188	0.6649	0.3380	0.4739	− 6.49	18
24	0.2373	0.4384	0.25	0.3960	0.4710	0.4	0.4223	− 7.49	22
25	0	0.2877	0.5	0.33	0.4124	0.5	0.4153	− 7.63	23

Table 5. Preprocessing data for each performance feature (gray relational generation).

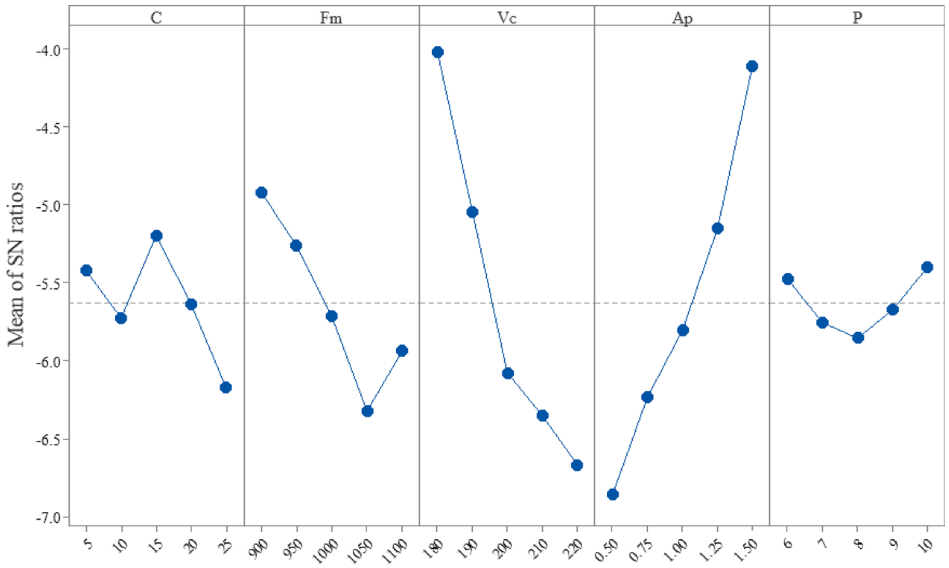

Fig. 10. S/N diagram for gray relational analysis.

Factors	DF	Seq SS	MS	F	P	Remarks
C	4	0.008331	0.002083	2.81	0.171	Insignificant
Vc	4	0.020143	0.005036	6.78	0.045	Significant
Fm	4	0.088523	0.022131	29.81	0.003	Significant
Ap	4	0.081072	0.020268	27.3	0.004	Significant
P	4	0.002345	0.000586	0.79	0.588	Insignificant
Error	4	0.00297	0.000742			
Total	24	0.203384				

Table 6. ANOVA Gray relational analysis.

ANOVA for grey relational grade

ANOVA is a statistical method used to detect the individual interactions of all the control factors in the experimental results. Significant machining parameters were identified using analysis of variance (ANOVA). ANOVA analysis was performed with a 95% confidence level and a 5% significance level. The F values of the control factors indicated the significance of the control factors by ANOVA analysis. The percentage contribution of each parameter is shown in the last column of the ANOVA table. This column demonstrates the extent to which the control factors influence the results. ANOVA aims to identify the effective parameters in milling that significantly affect the multiple responses. ANOVA was performed using gray relationship degree data, as shown in Table 6. Feed rate is considered the most significant factor from the ANOVA study, considering both flank wear and surface roughness simultaneously, as their P values are less than 0.05.The average GRG for each level of milling process parameters is presented in Table 7. Additionally, the average total gray relation grade for Test 25, as shown in Table 7, was calculated to be 0.5307.

$$\text{Total average value of gery relational grade} = 0.530695$$

The signal-to-noise ratio (often abbreviated as S/N) was used in conjunction with the Taguchi method to measure the variation in the experimental design. The term "signal" represents the desired effect on the responses, and "noise" represents the undesirable effect. Therefore, the maximum S/N ratio gives the optimal results for the responses. Three different methods for calculating the S/N ratio are nominal-best, smaller-better, and larger-better. This section utilized the larger-better S/N quality characteristic to obtain the optimal combination for optimizing multiple responses, as a higher GRG was desirable. The larger-better approach for a higher GRG is defined as follows:

$$S/N = -10log_{10}\left[\frac{1}{n}\left(\sum_{i=1}^{n}\frac{1}{y_i^2}\right)\right]. \quad (7)$$

In Eq. (7), yi is the ith measured test result in a run/row, and n describes the number of measurements in each test/row. Note that the target value of y/1 in the larger and better features is 0. The S/N ratio of multiple quality

Symbol	Parameter	Grey relational grade						
		Level 1	Level 2	Level 3	Level 4	Level 5	Delta	Rank
C	Concentration	0.5383	0.5266	**0.5574**	0.53	0.5011	0.0563	4
Vc	Cutting speed	**0.5729**	0.5516	0.5244	0.4933	0.5114	0.0796	3
Fm	Flow rate	**0.632**	0.5617	0.5057	0.4838	0.4702	0.1618	1
Ap	Depth of cut	0.4615	0.491	0.5186	0.5567	**0.6257**	0.1642	2
P	Pressure	0.5372	0.533	0.5123	0.5312	**0.5397**	0.0275	5

Table 7. Response table for GRG. Significant values are in [bold].

Input parameter	Concentration	Cutting speed	Feed rate	Depth of cut	Fluid pressure
Optimal value	15%	180 m/min	900 mm/min	1.5 mm	10 bar

Table 8. Optimal value of input parameters. Significant values are in [bold].

Initial cutting conditions			
		Prediction	Experiment
Level	C3-Vc2-Fm3-Ap1-P3	C3-Vc1-Fm1-Ap5-P5	C3-Vc1-Fm1-Ap5-P5
VB_{avg}	82.34		69.3
Ra	2.527		1.92
MRR	16.538		42.525
GRG	0.4606	0.8049	0.8322

Table 9. Validation results.

features was calculated using Eq. (6) and is listed in Table 5. The highest signal-to-noise ratio (S/N ratio) yields the best result. As can be seen in Fig. 10, at the highest S/N ratio of GRG, the optimal parametric combination was found to be C (level 3), Vc (level 1) and Fm (level 1), Ap (level 5) and P (level 5), The value of which is shown in Table 8.

Verification tests

In the final stage of Taguchi-based GRA, verification experiments were conducted using control factors at optimal and random levels to verify the accuracy of the optimization and determine the improvement in responses. Also, the verification experiments were repeated three times. Therefore, the estimated gray relation degree, i.e., the estimated at the optimal level of the design parameters, can be expressed as[49]:

$$\gamma_{estimated} = \gamma_m + \sum_{i=1}^{0} (\gamma_i - \gamma_m) \tag{8}$$

where $\gamma_{estimated}$ is the gray relation degree for predicting the optimal machining parameters, γ_m is the average of the total gray relation score, γ_i is the average gray relation degree at the optimal level, and o is the number of main design parameters significantly affecting the quality characteristics. Table 9 compares the estimated gray relation degree (0.8049) calculated by Eq. 8 and the experimental value (0.8322) obtained from the experiment at the optimal level. According to Table 9, there is a good agreement between the estimated value and the experimental value. It is found that the improvement of the gray relation degree from the initial factor combination (C3-Vc5-Fm2-Ap4-P1) to the optimal factor combination (C5-Vc5-Fm5-Ap2-P4) is 0.3716, and the improvement of the gray relation degree with multiple responses is 38.88%, which is in good agreement with the literature results[50].

Conclusion

The primary objective of this research is to bridge the knowledge gap concerning the machining of GTD450 stainless steel under MQL conditions. The methodological framework comprises a Taguchi design of experiments to efficiently assess the impact of key parameters on critical outputs, including metal removal rate, flank wear, and surface roughness. To reconcile these multiple and potentially conflicting responses, Grey Relational Analysis (GRA) was synergized with the Taguchi method for optimization. The statistical analysis was extended through Analysis of Variance (ANOVA) to identify significant factors affecting the Grey Relational Grade (GRG) and through response surface methodology to model the complex inter-parameter relationships.

The key findings are summarized as follows:

1. The results confirm that GTD450's high toughness leads to poor inherent machinability, which can be significantly mitigated through parameter optimization.
2. The experimental outcomes were significantly influenced by several variables, namely MQL oil concentration, feed rate, cutting speed, depth of cut, and fluid pressure.This highlights the crucial importance of meticulous parameter selection and optimization in milling GTD450.
3. Among the parameters, feed rate, cutting speed, and MQL oil concentration had a considerable effect on surface roughness. The feed rate was identified as the most dominant factor influencing flank wear and cutting tool life.
4. The depth of cut demonstrated a comparatively lesser influence on surface integrity. Consequently, to maximize MRR, it is advisable to operate at the highest depth of cut feasible within the machine's power constraints.
5. MQL oil concentration was found to improve surface roughness by up to 12% at lower cutting speeds, highlighting its critical role, although its efficacy diminishes at higher speeds.
6. Scanning Electron Microscopy (SEM) images revealed wear patterns on the chip surface and tool flank, identified as built-up edge (BUE), built-up lip (BUL), and abrasion wear.
7. An increase in MQL fluid pressure of up to 37.5% significantly improved tool wear, demonstrating that MQL parameters can exert an influence on tool life comparable to that of primary machining parameters.
8. The optimization process enhanced the Grey Relational Grade (GRG) from the initial parameter set to an optimized combination, achieving a final GRG of 0.3716.
9. This corresponded to a 38.8% improvement in the overall GRG, confirming that the Taguchi-based GRA approach successfully enhanced multiple performance indicators, including surface roughness and tool wear, for this difficult-to-machine material.
10. ANOVA of the GRG identified MQL oil concentration, fluid pressure, and cutting speed as the most significant parameters, with oil concentration being the most crucial factor for minimizing undesirable responses.
11. The use of an oil–water emulsion proved highly effective. An optimal MQL oil concentration of 15% was determined, with tool wear decreasing as concentration increased from 5% to this threshold, beyond which the benefits plateaued. Furthermore, surface roughness exhibited an inverse relationship with oil concentration, improving as the concentration was increased.
12. At constant cutting speed and feed, increased MQL pressure directly reduced both surface roughness and flank wear, confirming its significant role in enhancing surface finish and extending tool life.

Data availability

Data sets generated during the current study are available from the corresponding author on reasonable request.

Received: 7 July 2025; Accepted: 4 November 2025
Published online: 15 December 2025

References

1. Zhou, T. et al. Quantitative electron microscopy and physically based modelling of Cu precipitation in precipitation-hardening martensitic stainless steel 15-5 PH. *Mater. Des.* **143**, 141–149 (2018).
2. Khamseh, S. et al. Developing a graphite like carbon: Niobium thin film on GTD-450 stainless steel substrate. *Appl. Surf. Sci.* **511**, 145613 (2020).
3. DeMasi-Marcin, J. T. & Gupta, D. K. Protective coatings in the gas turbine engine. *Surf. Coat. Technol.* **68**, 1–9 (1994).
4. Poursaeidi, E. et al. Experimental investigation on erosion performance and wear factors of custom 450 steel as the first row blade material of an axial compressor. *Int. J. Surf. Sci. Eng.* **11**(2), 85–99 (2017).
5. Khamseh, S. et al. A tailored pulsed substrate bias voltage deposited (aC: Nb) thin-film coating on GTD-450 stainless steel: Enhancing mechanical and corrosion protection characteristics. *Chem. Eng. J.* **404**, 126490 (2021).
6. Nair, A. et al. Research developments and technological advancements in conventional and non-conventional machining of superalloys—A review. *J. Adhes. Sci. Technol.* **37**(22), 3053–3124 (2023).
7. Tayal, A., Kalsi, N. S. & Gupta, M. K. Machining of superalloys: A review on machining parameters, cutting tools, and cooling methods. *Mater. Today Proc.* **43**, 1839–1849 (2021).
8. Bijanzad, A., Munir, T. & Abdulhamid, F. Heat-assisted machining of superalloys: A review. *Int. J. Adv. Manuf. Technol.* **118**(11), 3531–3557 (2022).
9. Madhukar, S. et al. A critical review on minimum quantity lubrication (MQL) coolant system for machining operations. *Int. J. Curr. Eng. Int. J. Curr. Eng. Technol.* **6**(5), 1745–1751 (2016).
10. Niknam, S. A., et al. Ultrafine and fine particle emission in turning titanium metal matrix composite (Ti-MMC). 2019.
11. Altaf, S. F. et al. Machining with minimum quantity lubrication and nano-fluid MQL: A review. *Tribol. Online* **19**(3), 209–217 (2024).
12. Ali, S. H. et al. Recent developments in MQL machining of aeronautical materials: A comparative review. *Chin. J. Aeronaut.* **38**(1), 102918 (2025).
13. Iruj, M. et al. State-of-the-art hybrid lubrication (Cryo-MQL) supply systems, performance evaluation, and optimization studies in various machining processes. *Results Eng.* **22**, 102090 (2024).
14. Jouini, N. et al. Optimized machining parameters for high-speed turning process: A comparative study of dry and Cryo+ MQL techniques. *Processes* **13**(3), 739 (2025).
15. Li, D. et al. A comprehensive review of minimum quantity lubrication (MQL) machining technology and cutting performance. *Int. J. Adv. Manuf. Technol.* **133**(5), 2681–2707 (2024).
16. Ge, J. et al. Thermal effect in CFRP machining: Temperature field characteristics, heat generation mechanism and thermal damage management. *Compos. Struct.* **356**, 118845 (2025).
17. Resende, A. A. D. & Gonçalves dos Santos, A. Combination of minimum quantity lubrication (MQL) with solid lubricant (SL): Challenges, predictions and implications for sustainability. *Mach. Sci. Technol.* **28**(5), 777–818 (2024).
18. Kumar, S. et al. A comprehensive study on minimum quantity lubrication. *Mater. Today Proc.* **56**, 3078–3085 (2022).
19. Salur, E. et al. The effects of MQL and dry environments on tool wear, cutting temperature, and power consumption during end milling of AISI 1040 steel. *Metals* **11**(11), 1674 (2021).

20. Mia, M. et al. Taguchi S/N based optimization of machining parameters for surface roughness, tool wear and material removal rate in hard turning under MQL cutting condition. *Measurement* **122**, 380–391 (2018).
21. Kazeem, R. A. et al. Advances in the application of vegetable-oil-based cutting fluids to sustainable machining operations—A review. *Lubricants* **10**(4), 69 (2022).
22. Shewakh, W., Faqihi, A. A. & Ibrahem, R. Natural oils as an eco-friendly lubricant for machining operations, a review. *J. Egypt. Soc. Tribol.* **21**(1), 78–90 (2024).
23. Saravanan, R. et al. Performance assessment of non-edible vegetable oil blends in drilling AISI 1050 via minimum quantity lubrication. *J. Tribol.* **44**, 200–215 (2025).
24. Elmunafi, M. H. S., Noordin, M. & Kurniawan, D. Tool life of coated carbide cutting tool when turning hardened stainless steel under minimum quantity lubricant using castor oil. *Procedia Manuf.* **2**, 563–567 (2015).
25. Shankar, S., Mohanraj, T. & Ponappa, K. Influence of vegetable based cutting fluids on cutting force and vibration signature during milling of aluminium metal matrix composites. *J. Tribol.* **12**, 1–17 (2017).
26. Bedi, S. S., Behera, G. C. & Datta, S. Effects of cutting speed on MQL machining performance of AISI 304 stainless steel using uncoated carbide insert: Application potential of coconut oil and rice bran oil as cutting fluids. *Arab. J. Sci. Eng.* **45**, 8877–8893 (2020).
27. Chandel, R. S., Kumar, R. & Kapoor, J. Sustainability aspects of machining operations: A summary of concepts. *Mater. Today Proc.* **50**, 716–727 (2022).
28. Obikawa, T., Asano, Y. & Kamata, Y. Computer fluid dynamics analysis for efficient spraying of oil mist in finish-turning of Inconel 718. *Int. J. Mach. Tools Manuf* **49**(12–13), 971–978 (2009).
29. Stachurski, W. et al. Influence of application of hybrid MQL-CCA method of applying coolant during hob cutter sharpening on cutting blade surface condition. *J. Clean. Prod.* **171**, 892–910 (2018).
30. Gupta, A. et al. Sustainable machining using hybrid nanofluids under minimum quantity lubrication (MQL). *Adv. Ind. Prod. Eng. Sel. Proc. FLAME* **2019**, 573–584 (2018).
31. Gupta, M. K. et al. Ecological, economical and technological perspectives based sustainability assessment in hybrid-cooling assisted machining of Ti–6Al–4V alloy. *Sustain. Mater. Technol.* **26**, e00218 (2020).
32. Said, Z. et al. A comprehensive review on minimum quantity lubrication (MQL) in machining processes using nano-cutting fluids. *Int. J. Adv. Manuf. Technol.* **105**, 2057–2086 (2019).
33. Pereira, R. B. D. et al. Hybrid cryogenic/MQL helical milling for hole-making of Inconel 718. *Results Eng.* **26**, 104776 (2025).
34. Khanna, N. et al. Review on design and development of cryogenic machining setups for heat resistant alloys and composites. *J. Manuf. Process.* **68**, 398–422 (2021).
35. Sharif, M. N., Pervaiz, S. & Deiab, I. Potential of alternative lubrication strategies for metal cutting processes: A review. *Int. J. Adv. Manuf. Technol.* **89**, 2447–2479 (2017).
36. Zeilmann, R. P. & Weingaertner, W. L. Analysis of temperature during drilling of Ti_6Al_4V with minimal quantity of lubricant. *J. Mater. Process. Technol.* **179**(1–3), 124–127 (2006).
37. Boubekri, N., Shaikh, V. & Foster, P. R. A technology enabler for green machining: Minimum quantity lubrication (MQL). *J. Manuf. Technol. Manag.* **21**(5), 556–566 (2010).
38. Hamran, N. N. et al. A review on recent development of minimum quantity lubrication for sustainable machining. *J. Clean. Prod.* **268**, 122165 (2020).
39. Sarma, D. et al. Material-specific machining optimization of Ti_6Al_4V alloy under MQL: A sustainability-centric approach. *Next Mater.* **8**, 100586 (2025).
40. Liu, N. et al. Optimization of MQL turning process considering the distribution and control of cutting fluid mist particles. *Int. J. Adv. Manuf. Technol.* **116**, 1233–1246 (2021).
41. Zadafiya, K. et al. Recent advancements in nano-lubrication strategies for machining processes considering their health and environmental impacts. *J. Manuf. Process.* **68**, 481–511 (2021).
42. Gajrani, K. K. et al. Thermal, rheological, wettability and hard machining performance of MoS_2 and CaF_2 based minimum quantity hybrid nano-green cutting fluids. *J. Mater. Process. Technol.* **266**, 125–139 (2019).
43. Zaman, P. B., Tusar, M. I. H. & Dhar, N. R. Selection of appropriate process inputs for turning Ti–6Al–4V alloy under hybrid Al_2O_3-MWCNT nano-fluid based MQL. *Adv. Mater. Process. Technol.* **8**(1), 380–400 (2022).
44. Kumar, A., Sharma, A. & Katiyar, J. State-of-the-art in sustainable machining of different materials using nano minimum quality lubrication (NMQL). *Lubricants* **11**, 64 (2023).
45. Saberi, M., Niknam, S. A. & Hashemi, R. On the impacts of cutting parameters on surface roughness, tool wear mode and size in slot milling of A356 metal matrix composites reinforced with silicon carbide elements. *Proc. Inst. Mech. Eng. Part B J. Eng. Manuf.* **235**(10), 1655–1667 (2021).
46. Saberi, M., Niknam, S. A. & Hashemi, R. Characterizing the tool wear morphologies and life in milling A520–10% SiC under various lubrication and cutting conditions. *Sci. Rep.* **14**(1), 26870 (2024).
47. Dean, A. & Voss, D. *Design and Analysis of Experiments* (Springer, 1999).
48. Julong, D. Introduction to grey system theory. *J. Grey Syst.* **1**(1), 1–24 (1989).
49. Sahoo, A. K. & Sahoo, B. Performance studies of multilayer hard surface coatings (TiN/TiCN/Al_2O_3/TiN) of indexable carbide inserts in hard machining: Part-II (RSM, grey relational and techno economical approach). *Measurement* **46**(8), 2868–2884 (2013).
50. Sarıkaya, M. & Güllü, A. Multi-response optimization of minimum quantity lubrication parameters using Taguchi-based grey relational analysis in turning of difficult-to-cut alloy Haynes 25. *J. Clean. Prod.* **91**, 347–357 (2015).

Author contributions

Validation, M.S.; formal analysis, M.S.; investigation, M.S., SA.N.,A.H.,B.D.,R.H; writing—original draft preparation, M.S., SA.N.,A.H.,B.D.,R.H, supervision and writing—review and editing, M.S., SA.N.,A.H.,B.D.,R.H. All authors have read and agreed to the published version of the manuscript.

Declarations

Competing interests

The authors declare no competing interests.

Additional information

Correspondence and requests for materials should be addressed to S.A.N.